NeuroImage: Clinical 2 (2013) 151–160

Contents lists available at ScienceDirect

NeuroImage: Clinical

journal homepage: www.elsevier.com/locate/ynicl

Structural imaging differences and longitudinal changes in primary lateral sclerosis and amyotrophic lateral sclerosis☆

Justin Y. Kwan [1], Avner Meoded, Laura E. Danielian, Tianxia Wu, Mary Kay Floeter *

National Institute of Neurological Disorders and Stroke, National Institutes of Health, Bethesda, MD, USA

ARTICLE INFO

Article history:
Received 4 August 2012
Received in revised form 19 November 2012
Accepted 12 December 2012
Available online 24 December 2012

Keywords:
Cortical thickness
Longitudinal studies
Motor neuron disease
Diffusion tensor imaging
FreeSurfer

ABSTRACT

Magnetic resonance imaging measures have been proposed as objective markers to study upper motor neuron loss in motor neuron disorders. Cross-sectional studies have identified imaging differences between groups of healthy controls and patients with amyotrophic lateral sclerosis (ALS) or primary lateral sclerosis (PLS) that correlate with disease severity, but it is not known whether imaging measures change as disease progresses. Additionally, whether imaging measures change in a similar fashion with disease progression in PLS and ALS is unclear. To address these questions, clinical and imaging evaluations were first carried out in a prospective cross-sectional study of 23 ALS and 22 PLS patients with similar motor impairment and 19 age-matched healthy controls. Clinical evaluations consisted of a neurological examination, the ALS Functional rating scale-revised, and measures of finger tapping, gait, and timed speech. Age and ALSFRS score were not different, but PLS patients had longer duration of symptoms. Imaging measures examined were cortical thickness, regional brain volumes, and diffusion tensor imaging of the corticospinal tract and callosum. Imaging measures that differed from controls in a cross-sectional vertex-wise analysis were used as regions of interest for longitudinal analysis, which was carried out in 9 of the ALS patients (interval 1.26 ± 0.72 years) and 12 PLS patients (interval 2.08 ± 0.93 years). In the cross-sectional study both groups had areas of cortical thinning, which was more extensive in motor regions in PLS patients. At follow-up, clinical measures declined more in ALS than PLS patients. Cortical thinning and grey matter volume loss of the precentral gyri progressed over the follow-up interval. Fractional anisotropy of the corticospinal tracts remained stable, but the cross-sectional area declined in ALS patients. Changes in clinical measures correlated with changes in precentral cortical thickness and grey matter volume. The rate of cortical thinning was greater in ALS patients with shorter disease durations, suggesting that thickness decreases in a non-linear fashion. Thus, cortical thickness changes are a potential imaging marker for disease progression in individual patients, but the magnitude of change likely depends on disease duration and progression rate. Differences between PLS and ALS patients in the magnitude of thinning in cross-sectional studies are likely to reflect longer disease duration. We conclude that there is an evolution of structural imaging changes with disease progression in motor neuron disorders. Some changes, such as diffusion properties of the corticospinal tract, occur early while cortical thinning and volume loss occur later.

1. Introduction

Amyotrophic lateral sclerosis (ALS) and primary lateral sclerosis (PLS) are clinically distinct motor neuron disorders. Both disorders, however, are characterized by the progressive dysfunction and loss of corticospinal, or upper, motor neurons (UMNs). Although clinical signs are used to diagnose UMN dysfunction, they provide limited information about the severity of UMN loss. Several types of tests have been proposed as objective measures of UMN dysfunction (Bowser et al., 2006; Kaufmann et al., 2004; Turner and Modo, 2010; Ziemann et al., 1997). Among these, magnetic resonance imaging (MRI) of the brain has received the most widespread acceptance as a potential method to quantify UMN dysfunction (Turner et al., 2011, 2012). Quantitative imaging methods, including volumetric measures (Tartaglia et al., 2009; Thivard et al., 2007), diffusion tensor imaging (DTI) (Agosta et al., 2010a; Ellis

Abbreviations: ALS, amyotrophic lateral sclerosis; ALSFRS-R, ALS functional rating scale, revised; CC, corpus callosum; CST, corticospinal tract; DTI, diffusion tensor imaging; FA, fractional anisotropy; MD, mean diffusivity; MRI, magnetic resonance imaging; PLS, primary lateral sclerosis; UMN, upper motor neuron.

* Corresponding author at: 10 Center Drive MSC 1404, Building 10 CRC Room 7-5680, Bethesda MD 20892-1404, USA. Tel.: +1 301 496 7428; fax: +1 301 402 8796.
E-mail address: floeterm@ninds.nih.gov (M.K. Floeter).
[1] Current address: Department of Neurology, School of Medicine, University of Maryland, 110 South Paca Street, 3rd Floor, Baltimore MD 21201, USA.

2213-1582/$ – see front matter © 2012 The Authors. Published by Elsevier Inc. All rights reserved.
http://dx.doi.org/10.1016/j.nicl.2012.12.003

et al., 1999; Iwata et al., 2008, 2011), magnetic resonance spectroscopy (Mitsumoto et al., 2007; Pyra et al., 2010), and resting state functional MRI (Agosta et al., 2011, 2012a; Verstraete et al., 2010), show differences between healthy controls and patients with ALS or PLS. In cross-sectional studies of ALS patients, some imaging measures correlated with measures of disease severity. For example, within a group of ALS patients, the fractional anisotropy (FA) of the corticospinal tract in DTI studies was correlated with scores on the ALS functional rating scale (ALSFRS-R) and with central motor conduction time (Ellis et al., 1999; Iwata et al., 2008). From such data it has been suggested that the FA of the corticospinal tract could serve as a marker of clinical progression.

However, it has not been established that quantitative MRI measures change with clinical progression in individual patients. Only a small number of patients have been studied longitudinally; the relationship between imaging findings and clinical measures has largely been inferred from cross-sectional studies. The relationship between FA and clinical function may be complex. We found that PLS patients had reduced corticospinal tract FA, but unlike ALS patients in the same study, measures of corticospinal FA were not correlated with measures of UMN function; in PLS patients clinical measures correlated better with the mean diffusivity (MD) of the corticospinal tract (Iwata et al., 2011). We wondered if such differences between PLS and ALS patients were related to differences in disease duration or reflected differences in their underlying biology. In ALS, the median survival is 3–5 years from the time of diagnosis (Czaplinski et al., 2006), whereas the median survival in PLS is often several decades long (Floeter and Mills, 2009; Tartaglia et al., 2007).

On the other hand, imaging measures could differ between ALS and PLS because of differing pathology. A leading hypothesis is that both disorders lie on the same disease continuum with a common pathology characterized by neuronal loss and intra-neuronal inclusions, and that the different clinical phenotypes are caused by regional differences in the burden of pathology. Autopsy studies of ALS brains have found that neuronal inclusions containing TDP-43 extend to extra-motor cortical regions (Geser et al., 2008). This raises the question whether PLS patients have a more restricted phenotype because of a more restricted distribution of pathology. Because there are few post-mortem studies of PLS patients, it is difficult to test this hypothesis directly. MRI offers a non-invasive alternative to look for affected brain regions of living PLS and ALS patients. To date, only a few imaging studies have directly compared cohorts of patients with PLS to patients with ALS (Ciccarelli et al., 2009; Iwata et al., 2011).

The first part of the study addressed the hypothesis that affected regions of the brain differ between PLS and ALS patients, as would be consistent with a differential distribution of pathology. Imaging measures that potentially could reflect pathological changes, such as cortical thickness and volumes of grey and white matter tracts, were assessed in a cross-sectional study comparing brain MRIs from patients to age-matched healthy controls. To first visualize areas of cortical thinning, an unbiased whole-brain vertex-wise comparison was carried out. Measures of the cortical thickness and grey and white volumes of the regions of interest identified in that unbiased analysis were then compared between the patient groups. The second question examined was whether changes in imaging measures correlated with clinical progression. Approximately half of the patients in the cross-sectional study were able to participate in longitudinal imaging studies. In this subset of patients, we looked at the correlations between changes in clinical and imaging measures, focusing on regions of interest identified in the cross-sectional study and white matter tracts previously identified with clinical severity (Agosta et al., 2010a, 2012b; Ellis et al., 1999; Iwata et al., 2011).

2. Methods

2.1. Subjects

Twenty-two patients who fulfilled Pringle's criteria for PLS (Pringle et al., 1992), 23 patients with clinical probable or definite ALS by revised El Escorial criteria (Brooks et al., 2000), and 19 age-matched healthy controls participated in the cross-sectional study. All subjects gave written, informed consent for the protocol, which was approved by the Institutional Review Board. Some of these patients also participated in a previously reported diffusion tensor imaging study (Iwata et al., 2011). A subset of 12 PLS and 9 ALS patients who did not develop contraindications to MRI or significant respiratory or bulbar dysfunction had longitudinal clinical evaluations and neuroimaging studies. The interval between scans was longer for PLS patients than for ALS patients in order to allow measureable clinical progression between scans.

2.2. Clinical evaluation

A detailed history was obtained to determine the site of onset, progression of symptoms, and duration of disease. Patients and caregivers were questioned about behavior that would indicate cognitive changes or frontotemporal dysfunction. Most patients had neuropsychological testing. None of the patients had frontotemporal dementia or a family history of ALS or frontotemporal dementia. All ALS and PLS patients underwent diagnostic testing to confirm that they fulfilled the El Escorial criteria for probable or definite ALS (Brooks et al., 2000) or the Pringle criteria for PLS (Pringle et al., 1992). At each visit, a neurologist performed a neurological examination on all subjects. All healthy controls had normal neurological examinations. The revised ALS Functional Rating Scale (ALSFRS-R) was recorded for all subjects (Cedarbaum et al., 1999). Finger tapping speed, time to walk 20 feet, and time to read a standard passage were measured to quantify motor function. At the first evaluation 4 patients were unable to speak, 4 were unable to tap fingers, and 7 patients were unable to walk. For statistical analysis, in patients who were unable or became unable to perform these tasks, a value of zero was imputed for finger tapping and a value one second greater than that of the most severely affected patient was imputed for speech and gait. Although the true measures of motor function are unknown, this is a conservative method for imputing values. The rate of disease progression from onset of symptoms to the first study evaluation was estimated by the following calculation: (48 – ALSFRS-*R* score at first clinical evaluation)/time in months between first symptom and first study evaluation. The rate of disease progression during the follow-up interval was calculated as follows: (ALSFRS-*R* score at first time point evaluation – ALSFRS-*R* score at last time point)/follow-up interval in months.

2.3. Magnetic resonance imaging analysis

Magnetic resonance imaging (MRI) studies were performed on a 3 T scanner (Philips Achieva, Best, the Netherlands) using a receive-only, eight-channel SENSE head coil. For volumetric and thickness measurements, a high resolution T1-weighted image was obtained using a three dimensional turbo field echo sequence (3D T1 TFE) with TR = 8.6 ms, TE = 3.9 ms, TI = 700 ms, flip angle = 6°, FOV = 240 mm, matrix size = 256 × 256, slice thickness = 1 mm and 140 axial slices. For DTI studies, multi-slice diffusion weighted imaging was acquired with diffusion weighting along 32 non-collinear directions (b = 1000 s/mm2) and one volume without diffusion gradients applied (b0). The sequence was repeated 4 times to increase the signal to noise ratio (TE = 86 ms, FOV = 240 mm, matrix size = 96 × 96 reconstructed to 128 × 128, voxel size = 1.875 mm × 1.875 mm × 2.5 mm, slice thickness = 2.5 mm, and 55 contiguous axial slices aligned parallel to the AC-PC line).

Cortical reconstruction and volumetric segmentation was performed with the FreeSurfer image analysis suite (http://surfer.nmr.mgh.harvard.edu/). The technical details of these procedures have been described and validated in prior publications (Dale et al., 1999; Fischl and Dale, 2000; Fischl et al., 1999a, 1999b). Briefly, the processing included skull stripping, Talairach transformation, optimization of the grey matter-white matter and grey matter–CSF boundaries, segmentation, and tessellation

(Dale et al., 1999; Fischl and Dale, 2000). The tessellated surfaces were then inflated and registered to a spherical atlas which allowed for parcellation of the cerebral cortex into units based on gyral and sulcal structure, and creation of surface based data, including maps of curvature and sulcal depth (Fischl et al., 1999a, 1999b). Cortical thickness was calculated as the closest distance from the grey/white boundary to the grey/CSF boundary at each vertex on the tessellated surface (Fischl and Dale, 2000). Cortical gyri were parcellated as described by Desikan et al. (2006) for region-of-interest analyses. To measure changes in cortical thickness and volume between the initial and follow-up scans, images were processed using the longitudinal stream in FreeSurfer (http://surfer.nmr.mgh.harvard.edu/fswiki/LongitudinalProcessing) (Reuter et al., 2012). Briefly, this processing steam creates an unbiased within-subject template space and image using a robust inverse consistent registration (Reuter et al., 2010). Skull stripping, Talairach transformation, spherical maps, and parcellation are then initialized from the within-subject template for each subject's time point, utilizing common information and thereby increasing reliability and statistical power (Reuter et al., 2012).

Diffusion tensor imaging, and measurements of diffusion properties by fiber tracking, were carried out using methods previously described (Danielian et al., 2010; Iwata et al., 2011). Initial image processing, including eddy current correction, linear registration, and masking, was performed using FSL (University of Oxford, UK) (Smith et al., 2004). The diffusion tensor was calculated and fiber tracking was done using DtiStudio (Jiang et al., 2006) (www.MriStudio.org) using the Fiber Assignment by Continuous Tracking (FACT) method (Mori et al., 1999; Xue et al., 1999) with a minimum FA value of 0.2 for tracking termination and maximum 40 degree angle between two adjacent eigenvectors. The corticospinal tract (CST) was tracked using a multiple region-of-interest (ROI) approach (Iwata et al., 2011; Wakana et al., 2007) previously shown to have good reliability for longitudinal studies (Danielian et al., 2010) and the corpus callosum (CC) was segmented into the motor fibers of the corpus callosum, genu and splenium according to the technique of Hofer and Frahm (2006). Whole-tract measures of mean fractional anisotropy (FA) and mean diffusivity (MD; 10^{-3} mm^2/s) were calculated within each delineated tract. To assess for changes in cross-sectional area along the rostro-caudal extent of the corticospinal tract, profiles of the mean cross-sectional area within the tracked CST in each axial slice were constructed as previously described (Iwata et al., 2011).

In addition, longitudinal changes in diffusion metrics of the CST in the same anatomic space were evaluated by an atlas-based method (Oishi et al., 2009). DTI data was processed with DiffeoMap and RoiEditor software (Jiang et al., 2006) (www.MriStudio.org). The images were normalized to the ICBM-DTI-81 coordinates (Mori et al., 2008) using 12-mode affine transformation. Subsequently, a non-linear transformation using dual-contrast large deformation diffeomorphic metric mapping (LDDMM) was applied to register the FA and Trace images to the 1 mm isotropic resolution template ($181 \times 217 \times 181$ matrix). Because both linear and non-linear transformations are reciprocal procedures, the inversely transformed WMPMI parcellation map was superimposed onto the original DTI metrics maps from each patient, leading to the parcellation of the brain into 176 anatomical structures. For segmentation, a threshold of FA < 0.2 and Trace > 0.0045 was applied to exclude grey matter and CSF from white matter on the corresponding images. FA and MD measures were analyzed in five anatomically defined regions of the CST parcellated by this atlas-based method, shown in Fig. 1.

2.4. Statistical analysis

All data in tables are presented as mean ± standard deviation. Basic descriptive statistics and statistical analyses were performed using SPSS Statistics version 17.0 or SAS version 9.2. For clinical measures, Box–Cox transformation was applied to timed speech (natural logarithm), gait measurements (inverse square root) and ALSFRS-*R* (square); Shapiro–Wilk was used to test normality (based on the residuals). Demographic and clinical data were compared between groups in the cross-sectional study by one-way unequal variance ANOVA with post hoc Tukey's test. In the longitudinal study, within-subject changes in clinical measures were determined using a mixed model, described below.

2.4.1. Cross-sectional imaging analysis

For the cross-sectional study, unbiased whole-brain statistical comparisons were performed with FreeSurfer's QDEC application (www.surfer.nmr.mgh.harvard.edu). Surface maps depicting regions with statistically significant differences in cortical thickness at each vertex across the entire cortical mantle were determined in QDEC with general linear models (GLMs) using $p < 0.001$ uncorrected as the threshold for a significant cluster. Pairwise comparisons were made between ALS patients, PLS patients and healthy controls. Age and gender were not included as covariates in the QDEC model because these measures did not differ between the groups. Volumes of grey and white matter regions in which thinning was identified by QDEC were compared with a one-way ANOVA with post hoc Tukey's test.

2.5. Longitudinal analysis

Cortical regions found to have reduced thickness in the cross-sectional QDEC analysis were used as regions-of-interest in the longitudinal subset. Cortical thickness, grey matter volume and white matter volume of those regions were assessed, as well as changes in the FA and MD of the corticospinal tract and mid-posterior portion of the corpus callosum. The change between the two visits in these imaging measures and clinical measures was tested by a mixed model with patient as random effect. The full model included visits, diagnosis, interaction of diagnosis by visit, age and scan interval (p-value of 0.1 used as model selection). For those clinical and imaging measures showing significant change between the two visits, a general linear model was applied to examine the within-subject correlation, which described an increase in a clinical measure within the individual that was associated with an increase (or decrease) in an imaging measure by removing the difference between subjects (Bland and Altman, 1995). When an interaction between a clinical measure and diagnosis was significant, the association analysis was applied to ALS and PLS groups separately.

Brains processed with the FreeSurfer longitudinal stream were analyzed in QDEC with diagnosis as a discrete factor and disease duration as the covariate to generate surface maps showing where rates of thinning (thickness2 − thickness1)/(time2 − time1) differed between diagnoses.

3. Results

3.1. Cross-sectional demographics and clinical testing

There were no differences in age or gender between the three groups in the cross-sectional study (Table 1, left panel). The ALSFRS-*R*, timed speech, gait, and finger tapping rate were significantly different between healthy controls and patients ($p < 0.001$), but did not differ between the two patient groups. As expected, the mean duration of disease was longer in the PLS group than in the ALS group and the rate of disease progression was less in PLS patients than ALS patients. In the subset of 21 patients who underwent longitudinal studies, the age and gender ratios were similar to the cross-sectional group, but there was a trend towards slightly better clinical measures and a slower initial rate of disease progression in this subset compared to the cross-sectional group as a whole (Table 1, right panel).

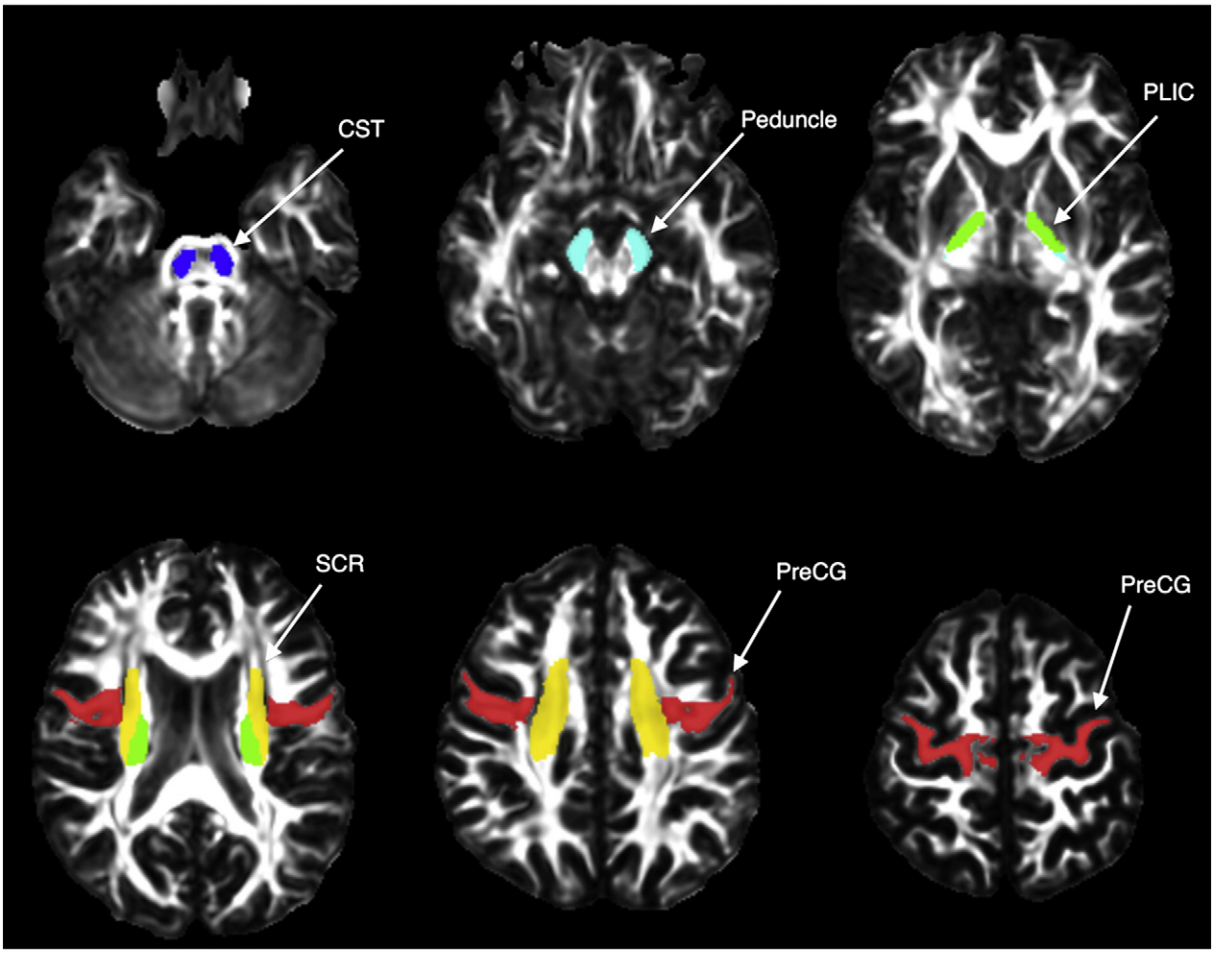

Fig. 1. Regions of the corticospinal tract defined by an atlas-based method that were used for longitudinal analysis of diffusion tensor imaging. Labeled regions include the pons (CST, blue), cerebral peduncle (Peduncle, turquoise), posterior limb of the internal capsule (PLIC, green), superior corona radiata (SCR, yellow), and the subcortical pre-central white matter (PreCG, red) (Oishi et al., 2009).

3.2. Cross-sectional imaging

3.2.1. Group differences in cortical thickness and grey and white matter volumes

Maps depicting pair-wise regional differences in cortical thickness between patients and healthy controls are shown in Fig. 2. In PLS patients cortical thinning was mostly limited to motor regions, with five clusters of thinning in the left precentral cortex and two clusters of thinning in the right precentral cortex (Fig. 2B). The coordinates of the maxima of the clusters in the precentral region corresponded approximately to Brodmann area 4 in Talairach space (Table 2) (Fischl et al., 2008). There was only one very small cluster of thinning outside of the motor area in PLS, in the left lateral orbital frontal region. In the ALS patients, clusters of cortical thinning were less extensive than in PLS patients (Fig. 2A). There were two clusters of cortical thinning in the left and right motor areas, with coordinates corresponding to Brodmann areas 4 and 6 in Talairach space (Table 2). Two clusters of cortical thinning occurred outside motor areas in ALS, in the left postcentral cortex and a small cluster in the rostral middle frontal cortex (Table 2). Based on these locations of thinning in the whole-brain maps, the following seven parcellated regions were selected for further region-of-interest analyses: right and left precentral gyrus, right and left paracentral region, left postcentral gyrus, left rostral middle frontal region, and left lateral orbital region.

The total brain, white, and grey matter volumes did not differ between groups (ANOVA, $p > 0.2$), indicating that there was no global atrophy. However, the grey and white matter volumes of some regions of interest, normalized for intracranial volume, differed between groups, suggesting focal atrophy (Supplementary Table 1). The right and left precentral grey matter volume was reduced in PLS and ALS patients and the grey matter of the post-central gyrus was reduced in ALS patients compared to controls. PLS patients also had reduced right and left precentral and paracentral white matter volume and ALS patients had reduced volume of the postcentral gyrus white matter.

3.3. Longitudinal study

3.3.1. Longitudinal changes in clinical and motor measures

Longitudinal evaluations were carried out in the subset of 9 ALS patients and 12 PLS patients who did not develop contraindications to MRI or significant respiratory dysfunction. The mean interval between follow-up evaluations was 1.26 ± 0.72 years for the ALS patients, and 2.08 ± 0.93 years for the PLS patients. Both groups exhibited a decline in the ALSFRS-*R* scores and in several of the motor measures over the follow-up interval, although the decline was more severe in the ALS patient group (Table 1, right panel). Mean ALSFRS-*R* scores declined by approximately 6 points in the ALS patient group and by 3.5 points in the PLS patient group. However, this includes five PLS patients who had stable ALSFRS-*R* scores that dropped one point or less. Measures of finger tapping speed declined bilaterally significantly in ALS patients over the follow-up interval. Two ALS patients became unable to perform one or more of the motor measures at follow-up that were initially performed. In PLS patients, only left-hand finger tapping exhibited

Table 1
Characteristics of subjects in cross-sectional study and longitudinal subset.

	Cross-sectional study			Longitudinal subset			
				PLS		ALS	
	Control	PLS	ALS	Initial	Follow-up	Initial	Follow-up
Male:Female	11:8	8:14	12:11	7:5		5:4	
Age (years)	58.7 ± 5.9	59.0 ± 7.9	55.8 ± 11.3	56.9 ± 9.4	59.41 ± 9.6	57.2 ± 12.6	58.38 ± 13.1
Disease duration (years)		[a]13.5 ± 6.7	3.0 ± 2.5	9.39 ± 4.2	11.87 ± 4.3	3.66 ± 2.9	4.87 ± 3.1
ALSFRS-*R*	[b]48.0 ± 0.0	36.3 ± 5.2	33.7 ± 7.1	39.8 ± 3.3	[c]36.2 ± 5.3	40.2 ± 6.3	[c]34.1 ± 9.8
Speech (s)	[b]51.1 ± 9.0	79.3 ± 26.9	84.3 ± 32.3	78.8 ± 26.0	81.8 ± 26.7	69.4 ± 31.7	85.2 ± 41.8
Gait (s)	[b]4.2 ± 0.7	21.4 ± 24.0	44.9 ± 49.5	12.4 ± 8.0	14.8 ± 11.1	24.9 ± 40.8	54.9 ± 57.1
Finger tapping R hand (taps/15 s)	[b]86.7 ± 12.7	48.4 ± 14.0	45.0 ± 32.5	51.0 ± 15.5	48.4 ± 13.3	63.0 ± 31.8	[c]23.0 ± 28.9
Finger tapping L hand (taps/15 s)	[b]85.1 ± 11.6	41.8 ± 14.2	43.4 ± 28.1	46.4 ± 15.0	[c]41.7 ± 13.00	57.4 ± 29.3	[c]23.2 ± 29.3
Progression rate*		[a]0.09 ± 0.06	0.77 ± 1.0	0.08 ± 0.04	0.14 ± 0.19	0.59 ± 1.26	0.51 ± 0.58

Follow-up progression rate = (ALSFRS-R1 − ALSFRS-R2) / follow-up interval in months.
[a] PLS and ALS significantly different, $p<0.05$.
[b] Controls significantly different from patients, $p<0.001$, no difference between PLS and ALS.
[c] Significant longitudinal change, $p<0.05$.
* Progression rate = (48-ALSFRS-*R*)/Disease duration in months.

significant, though modest, declines. There was a trend toward slower gait in both groups (ALS $p=0.053$; PLS $p=0.047$).

3.3.2. Longitudinal changes in diffusion tensor imaging

The corticospinal tract was analyzed both by a fiber tracking method and an atlas-based method. Fiber tracking showed a reduced mean FA and increased MD of the corticospinal tract compared to previously reported controls (Iwata et al., 2011), but the mean CST FA and MD remained relatively stable over the follow-up period, as illustrated for individual ALS and PLS patients (Supplementary Fig. 1). However, the mean cross-sectional area of the tracked CST became thinner along its rostro-caudal extent in the ALS patient group between the initial and follow-up evaluations (Fig. 3A). In PLS patients, the cross-sectional area of the CST remained stable over time (Fig. 3B). The atlas-based method likewise found no consistent pattern of change in the FA and MD measurements over the follow-up interval for the five regions of the corticospinal tract defined anatomically (Supplementary Fig. 2). The mid-portion of the corpus callosum, where fibers connecting the motor cortices travel (Hofer and Frahm, 2006) had lower FA and higher MD than previously published controls (Iwata et al., 2011), but the FA and MD remained stable during the follow-up interval in both patient groups (not shown).

3.3.3. Longitudinal changes in cortical thickness

Imaging measures from the two time points were obtained using the longitudinal processing stream in FreeSurfer (Reuter et al., 2012) and analyzed in SAS 9.2. Changes in the mean cortical thickness for each of the seven regions of interest (Table 2) were evaluated using a mixed model that included factors of age, scan interval, and diagnosis. PLS and ALS patients both had significant thinning of the right and left precentral gyrus between the two scans ($p<0.001$). There was a significant effect of the scan interval ($p<0.005$), with a greater degree of thinning when the interval between scans was longer. Significant thinning between scans also occurred in the left postcentral gyrus ($p=0.0095$) where thinning was affected by age ($p=0.0194$), but not by scan interval. Age did not significantly affect the thinning of the other regions studied.

To assess the effects of disease duration on the rate of thinning in ALS and PLS patients, a whole-brain vertex-wise analysis was carried out in QDEC using $p<0.001$ as the threshold for significance. The

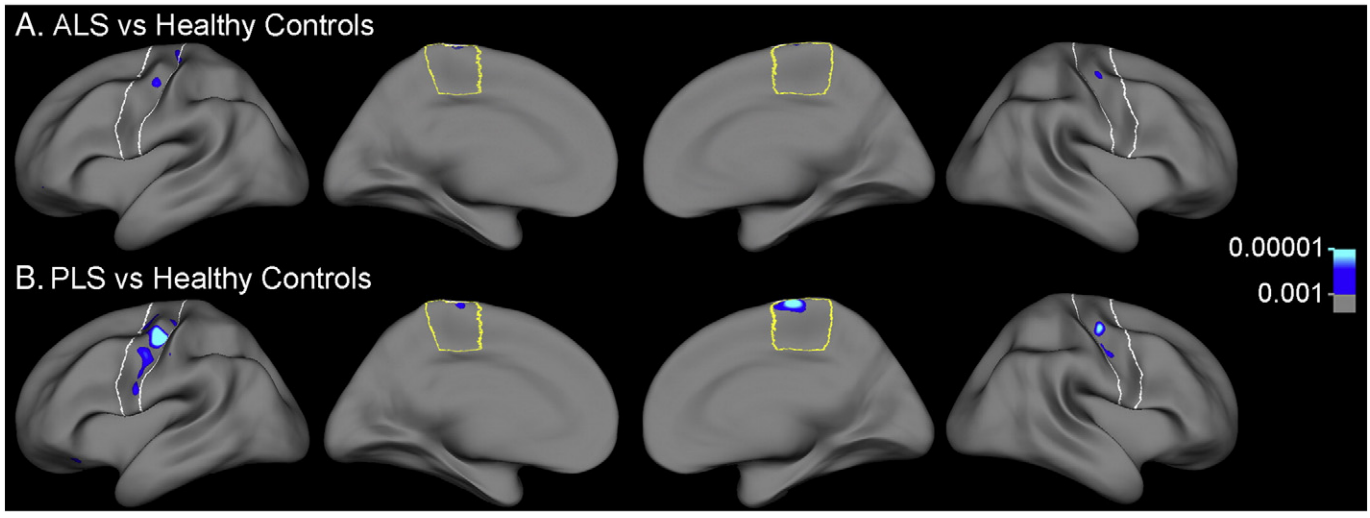

Fig. 2. Areas of cortical thinning identified in the cross-sectional study by a whole-brain vertex-wise analysis, shown projected on a smoothed average of all brains in this study. (FreeSurfer QDEC) Regions of thinning compared to healthy controls are shown for (A) ALS patients and (B) PLS patients. The color of the scale bar indicates the statistical significance of the cluster, ranging from the threshold value of $p<0.001$ to $p<0.00001$. White lines indicate the approximate region parcellated as precentral gyrus and the yellow lines indicate the region parcellated as paracentral region. Hemispheres are viewed from left to right as: left lateral, left medial, right medial, right lateral.

Table 2
Size and coordinates of clusters of cortical thinning in patients compared to controls identified in cross-sectional study vertex-wise analysis.

	Cluster size (mm^2)	Coordinate of maxima (Talairach coordinates)	FreeSurfer Region
PLS<Controls			
Left	273.4[a]	−32.8 −16.3 43.9	Precentral
	72.6[a]	−50.7 −5.4 41.7	Precentral
	23.4[a]	−57.6 2.2 22.3	Precentral
	15.3[a]	−25.9 −11.1 50.1	Precentral
	8.1[a]	−28.7 −21.4 49.3	Precentral
	1.8[a]	−30.5 28.4 −15.2	Lateral orbital frontal
Right	83.2[a]	5.6 −15.8 68.1	Precentral
	54.4[a]	36.3 −10.8 52.9	Precentral
ALS<Controls			
Left	64.5	−37.9 −10.3 46.8	Precentral
	40.7	−7.5 −21.6 69.0	Paracentral
	1.4	−39.9 49.6 −8.8	Rostral middle frontal
	84.0	−24.5 −26.9 53.8	Postcentral
Right	38.6	38.6 −9.2 55.5	Precentral
	6.1	5.4 −18.4 69.8	Paracentral
ALS>Controls			
Right	43.5	18.6 14.2 −19.3	Lateral orbital frontal

Threshold for significance was $p<0.001$ (uncorrected).
[a] Comparison also significant at $p<0.05$ with FDR correction for multiple comparisons.

resulting cortical maps showed five small areas where the average rates of thinning differed between ALS and PLS patients (Fig. 4A). These areas were located in the left and right precentral gyrus, the right paracentral region, the right superior frontal region, and the left cuneus region. For each of the five areas, the slope of the rate of thinning versus time from disease onset (using the mid-interval time point) differed for ALS patients and PLS patients. In ALS patients the rates of thinning in these areas was greatest in patients with a shorter disease duration, whereas the rates of thinning in PLS patients were similarly low in patients across the range of disease durations (Fig. 4B). Thickness of the right and left precentral cortex at each time point is shown for individual patients in Fig. 5 to further illustrate these differences.

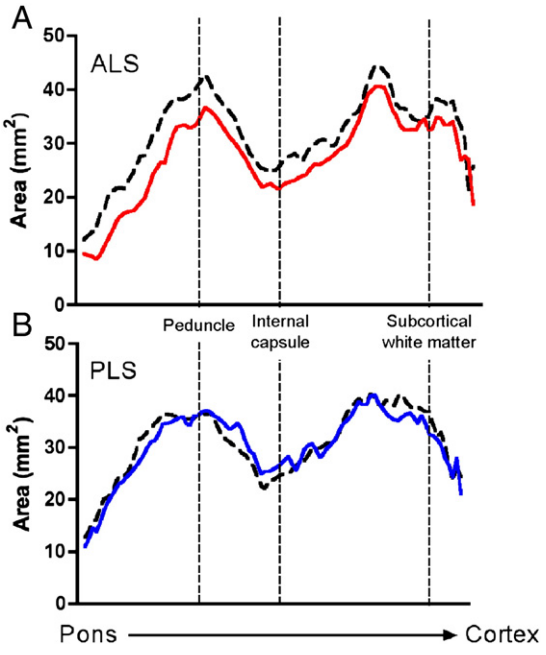

Fig. 3. Longitudinal changes in the cross-sectional area of the corticospinal tract. Dashed lines indicate the initial scan visit and solid colored lines indicate the follow-up. Fiber tracking was used to define the CST from the level of the mid-pons to the motor cortex and the two sides were averaged for the profiles. (A) In ALS patients, the cross-sectional area of the CST declined between the initial and follow-up evaluation. (B) In PLS patients, the CST cross-sectional area is smaller than in ALS, but there is no change during the follow-up interval. Dashed lines from left to right indicate three anatomic levels of the corticospinal tract: peduncle, internal capsule, and subcortical white matter.

3.3.4. Longitudinal changes in volumes of grey and white matter in regions of interest

In most of the regions with significant changes in cortical thickness, there generally was reduced volume of grey and white matter (Supplementary Table 2). The volume of grey matter declined in the precentral gyri bilaterally and the left postcentral gyrus in both ALS and PLS patients. Both groups also had loss of white matter volume in the left postcentral gyrus. PLS patients had loss of white matter volume in the precentral gyrus. There was also volume loss in the midposterior portion of the corpus callosum, adjusted for age. Age was not a significant factor in the volume loss observed in the other grey and white matter regions.

3.3.5. Correlation between longitudinal changes in clinical and imaging measures

Correlations were calculated between clinical and imaging measures that had significant declines over the follow-up interval. The decline in the ALSFRS-*R* score was correlated with thinning of the precentral cortex (left $r=0.459$, $p=0.036$; right $r=0.542$, $p=0.011$), loss of precentral grey matter volume (left $r=0.493$, $p=0.023$; right $r=0.560$, $p=0.011$), loss of left precentral white matter volume ($r=0.569$, $p=.007$), and loss of left postcentral white matter volume ($r=0.628$, $p=0.002$) in ALS and PLS patients. In PLS patients, the decline in left hand finger tapping speed was associated with a decline in right precentral cortex thickness ($r=0.586$, $p=0.036$) and grey matter volume ($r=0.644$, $p=0.0176$), with a trend toward an association with volume of the mid-posterior region of the corpus callosum ($r=0.522$, $p=0.067$). In ALS patients, the decline in right hand finger tapping rate was associated with a decline in the white matter of the postcentral gyrus ($r=0.713$, $p=0.0207$).

4. Discussion

There is a longstanding debate whether primary lateral sclerosis and amyotrophic lateral sclerosis are variants of the same disease (Rowland, 1999; Swash et al., 1999). Two characteristics that distinguish PLS from ALS are long survival and lack of significant lower motor neuron signs. Both disorders, however, have progressive upper motor neuron loss. In ALS, neuronal loss and pathological inclusions are widespread in the brain, but it is not known whether the same is true in PLS. The first part of this study compared the distribution of cortical thinning, a potential imaging marker of pathological change, in ALS and PLS patients to healthy controls in a whole-brain analysis. In the motor regions, cortical thinning occurred in a similar distribution in ALS and PLS patients, but the magnitude of thinning was greater in PLS patients. In PLS patients, cortical thinning was highly localized to the precentral gyrus and adjacent paracentral region, with only one very small cluster in the lateral orbitofrontal cortex. Thinning of the motor cortex is consistent with our earlier report in PLS patients using manual measurements of the precentral gyrus from T1 weighted MRI scans (Butman and Floeter, 2007), but that study did not examine the whole brain to look for changes in other regions. The current study did not find global atrophy in PLS patients, in contrast to a prior report (Tartaglia et al., 2009). However, in regions with large areas of thinning, i.e. the precentral cortex, the volumes of grey and white matter were less than in controls, indicating focal atrophy. Our findings do not support the hypothesis that cortical pathology is widespread in PLS patients. Despite their long duration of disease, imaging differences were mostly restricted to the motor regions in PLS and did not spread to adjacent cortical regions. Small areas of cortical thinning within

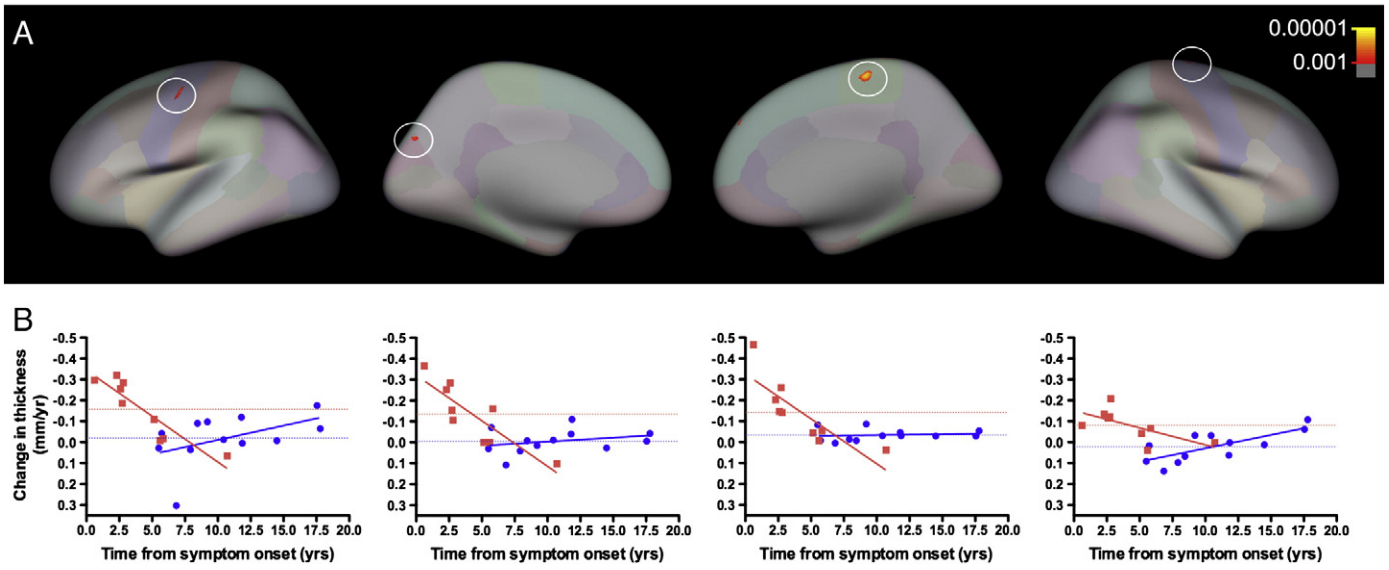

Fig. 4. Differences in rates of cortical thinning as a function of disease duration in PLS and ALS patients in a whole-brain vertex-wise analysis. (A) Regions where the average rate of change in thickness differs between ALS patients and PLS patients are shown on the smoothed average brain template (FreeSurfer QDEC). The color of the scale bar indicates the statistical significance of the cluster, ranging from the threshold value of $p<0.001$ to $p<0.00001$. Hemispheres are viewed from left to right as: left lateral, left medial, right medial, right lateral. (B) Plots show the relationship between the rate of change in thickness (mm/year) for ALS patients (red squares) and PLS patients (blue circles) and the time of symptom onset (disease duration at the mid-point of the interval between scans). Data from each plot corresponds to the region of significance that is circled in the brain image directly above in (A). ALS patients (red dashed lines) had a faster average rate of thinning for the circled region compared to PLS patients (blue dashed lines). The solid lines show the fitted slopes for each disease group. Rate of change in thickness (mm/years) = (thickness2 − thickness1) / (time2 − time1).

the precentral gyrus were seen in the ALS patient group, in agreement with other studies (Agosta et al., 2012b; Roccatagliata et al., 2009; Verstraete et al., 2012). Thinning was also seen in the postcentral gyrus and a small region in the rostral frontal cortex in ALS. In the precentral cortex and the postcentral gyrus, where clusters of thinning were largest in ALS, the volume was also reduced. Although thinning extended beyond the motor cortex in ALS, it was not as widespread as has been described in other reports (Agosta et al., 2012b; Verstraete et al., 2012). Although some of the differences between the studies can be attributed to differences in the statistical models and method for selecting regions of interest, another contributing factor may be that none of the ALS patients in the current study had dementia, which is associated with greater frontotemporal pathology (Strong and Yang, 2011).

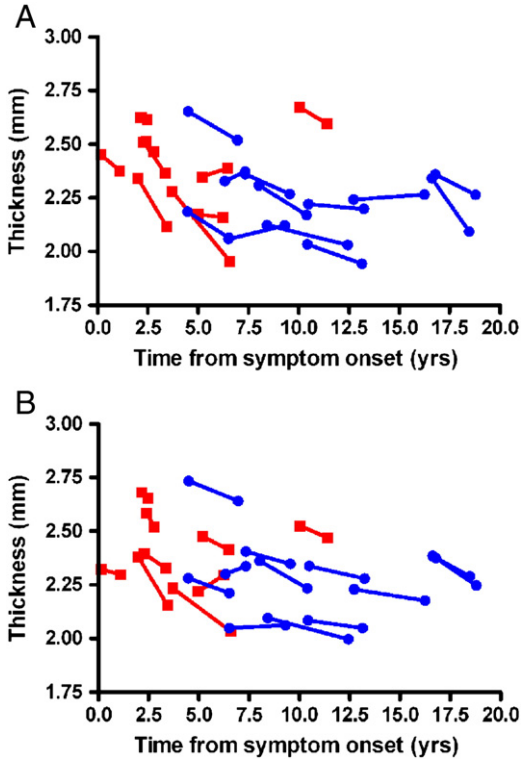

Fig. 5. Longitudinal changes in the mean cortical thickness of the precentral gyrus in patients with ALS (red squares) and PLS (blue circles). Time is referenced to the onset of the patient's symptoms. (A) Left precentral gyrus. (B) Right precentral gyrus.

The longitudinal portion of the study examined whether imaging measures change with clinical progression, focusing on the regions identified in the cross-sectional study. In the subset of patients who had longitudinal evaluations, cortical thinning was found to progress over time. After adjusting for covariates, in both ALS and PLS patients, only the precentral gyri showed significant interval change in thickness. The decline in thickness of the precentral cortex was correlated with a decline in the ALSFRS-*R* score. In PLS patients it also correlated with a decline in finger tapping speed. Thinning of the precentral cortex progressed at a faster rate in ALS patients than PLS patients, and within the group of ALS patients, more rapid thinning occurred in those with a shorter disease duration. In contrast, in PLS patients the rate of thinning was low and relatively similar across the range of disease durations. The different rates of thinning could reflect differences in the underlying disease processes in ALS and PLS. However, another interpretation of these data would be that thinning occurs in a non-linear fashion, with an early rapid phase of decline followed by a longer, slower phase of thinning, in a similar manner in both ALS and PLS patients. The detection of significant changes in thickness would therefore depend on the timing of the scans in relation to the disease duration and the patient's progression rate. Of note, however, is that patients with slower rates of progression may be over-represented in longitudinal studies, because they are more likely to tolerate repeat evaluations and are less likely to drop out than patients who have rapid progression of disease. This selection bias was true in the current study, as evidenced by the slower progression rates in the subset of patients who had follow-up imaging compared the whole group.

In the diffusion tensor imaging of the corticospinal tract, longitudinal changes occurred in cross-sectional area rather than in white matter diffusion properties. In this study, we analyzed the corticospinal tract by tractography and by an automated image parcellation/atlas-based analysis. Both methods yielded the same results, that changes in measures of corticospinal FA and MD did not correlate with changes in clinical measures. Tractography, or fiber tracking, depends on sufficient axonal integrity to produce directionality of diffusion for reconstructing tracts. Although fiber tracking of the corticospinal tract had high reliability in longitudinal studies of healthy controls (Danielian et al., 2010), it has the drawback that in patients with axonal disruption and loss, it can only assess surviving fibers. The fiber tracking method found that whole-tract measures of corticospinal tract diffusion properties were stable during the follow-up period in ALS and PLS patients, although they differed from control values at both time points. In ALS, the cross-sectional areas of the corticospinal tract declined between scans, presumably due to axonal loss and dropout of fibers from tracking. The atlas-based method is complementary to the fiber tracking method, as it assesses the brain in a structure-by-structure (group of pixels) basis using a common parcellation map. The method uses large deformation diffeomorphic metric mapping (LDDMM) as the normalization algorithm. The LDDMM has a high accuracy in matching the shapes of different brains to a standard atlas. The measurements acquired with the atlas-based analysis derive directly from the native images of each individual, reducing the imprecision produced by the imaging postprocessing. The atlas-based method showed no change in FA and MD of the corticospinal tract at the follow-up scan. Although the two methods did not find an interval change in diffusion properties, the patients' CST FA and MD differed from controls, indicating that changes in diffusion properties of the white matter tracts had already occurred prior to the time of the first scan. This finding that diffusion properties remained relatively stable differs from a study that found a decline in FA in the superior portion of the right corticospinal tract with a tractography-based region-of-interest analysis which divided each CST into three portions (Zhang et al., 2011). In that study, the changes were driven by a subset of patients with left-onset ALS (Zhang et al., 2011). This region is not well-tracked with our tractography method, which used a slightly higher FA threshold for truncation of tracking. Nevertheless, the atlas-based method also did not find changes in these regions. It is possible that the methods we used were not sensitive to small changes, particularly given the small sample size in the longitudinal study. Another possibility is that changes in CST diffusion properties occur very early in ALS, and thus were captured in the study by Zhang et al. (2011) where the mean disease duration of the group was 20.8 months, but not in our study where ALS patients had a mean disease duration of 36.6 months at the time of the first scan.

The tissue changes that give rise to imaging changes such as cortical thinning result from a remodeling process that requires time. In addition to shrinkage and loss of cortical neurons that could contribute to cortical thinning (Hudson et al., 1993; Kiernan and Hudson, 1991, 1993), there are also inflammatory changes with T-cell infiltration (Henkel et al., 2009), reactive astrocytosis (Murayama et al., 1991; Vargas and Johnson, 2010), microglia invasion (Turner et al., 2004), and iron accumulation (Kwan et al., 2012) in the cortex. These may contribute to a gradual thinning that continues beyond the period of neuronal loss, by clearing of necrotic debris and by maturation of glial scarring in patients who survive longer. This sequence of changes, and the time required for them to occur, would be consistent with the greater extent and degree of thinning of the motor cortex in PLS patients compared to ALS patients. A similar evolution of tissue changes in the white matter could also explain findings from diffusion tensor imaging studies. Nearly all cross-sectional diffusion tensor imaging studies have reported reduced fractional anisotropy of the corticospinal tract in ALS and PLS patients compared to healthy controls, and many studies found a correlation between the CST FA and clinical severity scores or progression rates (Ciccarelli et al., 2006, 2009; Ellis et al., 1999; Iwata et al., 2008, 2011; Mitsumoto et al., 2007; Sage et al., 2007; Ulug et al., 2004; Unrath et al., 2010). In the few longitudinal studies in ALS, lower corticospinal tract FA correlated with faster rates of disease progression or shorter survival, where ALS patients were followed for one (Nickerson et al., 2009) or up to approximately 3.5 years (Agosta et al., 2010b). The relatively short follow-up periods that can be achieved with ALS patients may not be sufficient to observe the full evolution of white matter changes that are seen in PLS patients, some of whom have decades-long disease durations. The changes in fractional anisotropy may be a relatively early event in motor neuron degeneration, during active degeneration of corticospinal axons, with loss of cross-sectional area of the tract occurring afterward. Others have also noted that diffusion properties can change independently of volumetric changes (Canu et al., 2011).

Several cross-sectional studies have reported differences in diffusion properties in motor fibers of the corpus callosum in ALS and PLS compared to healthy controls (Ciccarelli et al., 2009; Douaud et al., 2011; Iwata et al., 2011). It has been suggested that reduced fractional anisotropy in the mid-posterior corpus callosum is specific for ALS, and may precede the onset of clinical signs of upper motor neuron dysfunction (Filippini et al., 2010; Sach et al., 2004). This study confirms and extends that proposal, finding that the diffusion properties of the callosal motor fibers remained stable over the follow-up interval, although volume loss occurred. Thus the sequence of imaging changes in callosal fibers in motor neuron disease is similar to the corticospinal tract, with early changes in diffusion properties and later changes in volume.

This study's finding that progressive thinning and volume loss occurs primarily the precentral cortex is consistent with a longitudinal morphometry study that showed atrophy of the precentral region over a 9-month span in ALS patients (Agosta et al., 2009), but differs from a recent longitudinal study of ALS patients that found progressive thinning of extra-motor regions over a 3–10 month follow-up interval (Verstraete et al., 2012). One of the limitations of our longitudinal study is that the small sample sizes limited the number of regions that could be assessed in our statistical model. Regions of interest were selected from areas identified in the cross-sectional model which differed from age-matched controls, and did not include the whole brain. Of the three extra-motor regions assessed in our longitudinal model, only the postcentral gyrus showed progressive thinning in ALS patients. Several studies have reported more widespread atrophy in motor neuron disease (Grosskreutz et al., 2006; Tartaglia et al., 2009; Turner et al., 2007), including volume loss in the frontal and temporal lobes in patients with cognitive impairment (Chang et al., 2005; Strong et al., 2003). In our cross-sectional whole-brain analysis, a small cluster of thinning was seen in the lateral orbital frontal cortex in PLS patients, and small cluster of thinning occurred in the frontal cortex in ALS patients. The lack of more extensive findings in extramotor areas may reflect better cognitive function, as there is a selection bias in our study for patients who were able to travel to participate in research, compared to a more population-based cohort such as from a regional clinic (Grace et al., 2011; Murphy et al., 2008).

5. Conclusion

The findings from this longitudinal study favor the idea that there is a temporal evolution of imaging changes in the brain in motor neuron disorders as upper motor neuron degeneration progresses. We propose that alterations in the diffusion properties of the corticospinal tract and motor region of the corpus callosum are among the early changes, which eventually reach a nadir. Cortical thickness declines at a rapid rate initially, then at a slower rate, with progressive atrophy of the affected grey and white matter regions. Within this framework, longitudinal changes in imaging measures will be dependent on disease duration and progression rate and differences between ALS and PLS patients may be explained by differences in disease duration. Future studies with

larger sample sizes and additional longitudinal evaluations will be needed to test this proposed sequence of imaging changes. In the cross-sectional portion of this study, we found small differences between PLS and ALS patients in the distribution of cortical thinning, not a substantial differential distribution of pathology. However, this conclusion is limited by the clinical similarity of the two patient groups, with less widespread pathology in the ALS group than reported in other studies. A more diverse ALS patient sample should be studied to better assess regional differences between PLS and ALS. Lastly, we conclude that the imaging measure that best correlates with clinical progression is the decline in cortical thickness of the precentral gyrus.

Supplementary data to this article can be found online at http://dx.doi.org/10.1016/j.nicl.2012.12.003.

Funding

This work was supported by the Intramural Program of the National Institute of Neurological Disorders and Stroke, National Institutes of Health (Z01 NS002976).

Acknowledgments

The authors gratefully acknowledge Dr. John Ostuni for superb support with image processing.

References

Agosta, F., Gorno-Tempini, M.L., Pagani, E., Sala, S., Caputo, D., Perini, M., Bartolomei, I., Fruguglietti, M.E., Filippi, M., 2009. Longitudinal assessment of grey matter contraction in amyotrophic lateral sclerosis: a tensor based morphometry study. Amyotrophic Lateral Sclerosis 10, 168–174.

Agosta, F., Pagani, E., Petrolini, M., Caputo, D., Perini, M., Prelle, A., Salvi, F., Filippi, M., 2010a. Assessment of white matter tract damage in patients with amyotrophic lateral sclerosis: a diffusion tensor MR imaging tractography study. AJNR. American Journal of Neuroradiology 31, 1457–1461.

Agosta, F., Pagani, E., Petrolini, M., Sormani, M.P., Caputo, D., Perini, M., Prelle, A., Salvi, F., Filippi, M., 2010b. MRI predictors of long-term evolution in amyotrophic lateral sclerosis. European Journal of Neuroscience 32, 1490–1496.

Agosta, F., Valsasina, P., Absinta, M., Riva, N., Sala, S., Prelle, A., Copetti, M., Comola, M., Comi, G., Filippi, M., 2011. Sensorimotor functional connectivity changes in amyotrophic lateral sclerosis. Cerebral Cortex 21, 2291–2298.

Agosta, F., Canu, E., Valsasina, P., Riva, N., Prelle, A., Comi, G., Filippi, M., 2012a. Divergent brain network connectivity in amyotrophic lateral sclerosis. Neurobiology of Aging (May 17 [Epub ahead of print]).

Agosta, F., Valsasina, P., Riva, N., Copetti, M., Messina, M.J., Prelle, A., Comi, G., Filippi, M., 2012b. The cortical signature of amyotrophic lateral sclerosis. PLoS One 7, e42816.

Bland, J.M., Altman, D.G., 1995. Calculating correlation coefficients with repeated observations: Part 1—Correlation within subjects. BMJ 310, 446.

Bowser, R., Cudkowicz, M., Kaddurah-Daouk, R., 2006. Biomarkers for amyotrophic lateral sclerosis. Expert Review of Molecular Diagnostics 6, 387–398.

Brooks, B.R., Miller, R.G., Swash, M., Munsat, T.L., 2000. El Escorial revisited: revised criteria for the diagnosis of amyotrophic lateral sclerosis. Amyotrophic Lateral Sclerosis and Other Motor Neuron Disorders 1, 293–299.

Butman, J.A., Floeter, M.K., 2007. Decreased thickness of primary motor cortex in primary lateral sclerosis. AJNR. American Journal of Neuroradiology 28, 87–91.

Canu, E., Agosta, F., Riva, N., Sala, S., Prelle, A., Caputo, D., Perini, M., Comi, G., Filippi, M., 2011. The topography of brain microstructural damage in amyotrophic lateral sclerosis assessed using diffusion tensor MR imaging. AJNR. American Journal of Neuroradiology 32, 1307–1314.

Cedarbaum, J.M., Stambler, N., Malta, E., Fuller, C., Hilt, D., Thurmond, B., Nakanishi, A., 1999. The ALSFRS-R: a revised ALS functional rating scale that incorporates assessments of respiratory function. BDNF ALS Study Group (Phase III). Journal of Neurological Sciences 169, 13–21.

Chang, J.L., Lomen-Hoerth, C., Murphy, J., Henry, R.G., Kramer, J.H., Miller, B.L., Gorno-Tempini, M.L., 2005. A voxel-based morphometry study of patterns of brain atrophy in ALS and ALS/FTLD. Neurology 65, 75–80.

Ciccarelli, O., Behrens, T.E., Altmann, D.R., Orrell, R.W., Howard, R.S., Johansen-Berg, H., Miller, D.H., Matthews, P.M., Thompson, A.J., 2006. Probabilistic diffusion tractography: a potential tool to assess the rate of disease progression in amyotrophic lateral sclerosis. Brain 129, 1859–1871.

Ciccarelli, O., Behrens, T.E., Johansen-Berg, H., Talbot, K., Orrell, R.W., Howard, R.S., Nunes, R.G., Miller, D.H., Matthews, P.M., Thompson, A.J., Smith, S.M., 2009. Investigation of white matter pathology in ALS and PLS using tract-based spatial statistics. Human Brain Mapping 30, 615–624.

Czaplinski, A., Yen, A.A., Simpson, E.P., Appel, S.H., 2006. Slower disease progression and prolonged survival in contemporary patients with amyotrophic lateral sclerosis: is the natural history of amyotrophic lateral sclerosis changing? Archives of Neurology 63, 1139–1143.

Dale, A.M., Fischl, B., Sereno, M.I., 1999. Cortical surface-based analysis. I. Segmentation and surface reconstruction. NeuroImage 9, 179–194.

Danielian, L.E., Iwata, N.K., Thomasson, D.M., Floeter, M.K., 2010. Reliability of fiber tracking measurements in diffusion tensor imaging for longitudinal study. NeuroImage 49, 1572–1580.

Desikan, R.S., Segonne, F., Fischl, B., Quinn, B.T., Dickerson, B.C., Blacker, D., Buckner, R.L., Dale, A.M., Maguire, R.P., Hyman, B.T., Albert, M.S., Killiany, R.J., 2006. An automated labeling system for subdividing the human cerebral cortex on MRI scans into gyral based regions of interest. NeuroImage 31, 968–980.

Douaud, G., Filippini, N., Knight, S., Talbot, K., Turner, M.R., 2011. Integration of structural and functional magnetic resonance imaging in amyotrophic lateral sclerosis. Brain 134, 3470–3479.

Ellis, C.M., Simmons, A., Jones, D.K., Bland, J., Dawson, J.M., Horsfield, M.A., Williams, S.C., Leigh, P.N., 1999. Diffusion tensor MRI assesses corticospinal tract damage in ALS. Neurology 53, 1051–1058.

Filippini, N., Douaud, G., Mackay, C.E., Knight, S., Talbot, K., Turner, M.R., 2010. Corpus callosum involvement is a consistent feature of amyotrophic lateral sclerosis. Neurology 75, 1645–1652.

Fischl, B., Dale, A.M., 2000. Measuring the thickness of the human cerebral cortex from magnetic resonance images. Proceedings of the National Academy of Sciences of the United States of America 97, 11050–11055.

Fischl, B., Sereno, M.I., Dale, A.M., 1999a. Cortical surface-based analysis. II: Inflation, flattening, and a surface-based coordinate system. NeuroImage 9, 195–207.

Fischl, B., Sereno, M.I., Tootell, R.B., Dale, A.M., 1999b. High-resolution intersubject averaging and a coordinate system for the cortical surface. Human Brain Mapping 8, 272–284.

Fischl, B., Rajendran, N., Busa, E., Augustinack, J., Hinds, O., Yeo, B.T., Mohlberg, H., Amunts, K., Zilles, K., 2008. Cortical folding patterns and predicting cytoarchitecture. Cerebral Cortex 18, 1973–1980.

Floeter, M.K., Mills, R., 2009. Progression in primary lateral sclerosis: a prospective analysis. Amyotrophic Lateral Sclerosis 10, 339–346.

Geser, F., Brandmeir, N.J., Kwong, L.K., Martinez-Lage, M., Elman, L., McCluskey, L., Xie, S.X., Lee, V.M., Trojanowski, J.Q., 2008. Evidence of multisystem disorder in whole-brain map of pathological TDP-43 in amyotrophic lateral sclerosis. Archives of Neurology 65, 636–641.

Grace, G.M., Orange, J.B., Rowe, A., Findlater, K., Freedman, M., Strong, M.J., 2011. Neuropsychological functioning in PLS: a comparison with ALS. Canadian Journal of Neurological Sciences 38, 88–97.

Grosskreutz, J., Kaufmann, J., Fradrich, J., Dengler, R., Heinze, H.J., Peschel, T., 2006. Widespread sensorimotor and frontal cortical atrophy in amyotrophic lateral sclerosis. BMC Neurology 6, 17.

Henkel, J.S., Beers, D.R., Zhao, W., Appel, S.H., 2009. Microglia in ALS: the good, the bad, and the resting. Journal of Neuroimmune Pharmacology 4, 389–398.

Hofer, S., Frahm, J., 2006. Topography of the human corpus callosum revisited—comprehensive fiber tractography using diffusion tensor magnetic resonance imaging. NeuroImage 32, 989–994.

Hudson, A.J., Kiernan, J.A., Munoz, D.G., Pringle, C.E., Brown, W.F., Ebers, G.C., 1993. Clinicopathological features of primary lateral sclerosis are different from amyotrophic lateral sclerosis. Brain Research Bulletin 30, 359–364.

Iwata, N.K., Aoki, S., Okabe, S., Arai, N., Terao, Y., Kwak, S., Abe, O., Kanazawa, I., Tsuji, S., Ugawa, Y., 2008. Evaluation of corticospinal tracts in ALS with diffusion tensor MRI and brainstem stimulation. Neurology 70, 528–532.

Iwata, N.K., Kwan, J.Y., Danielian, L.E., Butman, J.A., Tovar-Moll, F., Bayat, E., Floeter, M.K., 2011. White matter alterations differ in primary lateral sclerosis and amyotrophic lateral sclerosis. Brain 134, 2642–2655.

Jiang, H., van Zijl, P.C., Kim, J., Pearlson, G.D., Mori, S., 2006. DtiStudio: resource program for diffusion tensor computation and fiber bundle tracking. Computer Methods and Programs in Biomedicine 81, 106–116.

Kaufmann, P., Pullman, S.L., Shungu, D.C., Chan, S., Hays, A.P., Del Bene, M.L., Dover, M.A., Vukic, M., Rowland, L.P., Mitsumoto, H., 2004. Objective tests for upper motor neuron involvement in amyotrophic lateral sclerosis (ALS). Neurology 62, 1753–1757.

Kiernan, J.A., Hudson, A.J., 1991. Changes in sizes of cortical and lower motor neurons in amyotrophic lateral sclerosis. Brain 114 (Pt 2), 843–853.

Kiernan, J.A., Hudson, A.J., 1993. Changes in shapes of surviving motor neurons in amyotrophic lateral sclerosis. Brain 116 (Pt 1), 203–215.

Kwan, J.Y., Jeong, S.Y., Van Gelderen, P., Deng, H.X., Quezado, M.M., Danielian, L.E., Butman, J.A., Chen, L., Bayat, E., Russell, J., Siddique, T., Duyn, J.H., Rouault, T.A., Floeter, M.K., 2012. Iron accumulation in deep cortical layers accounts for MRI signal abnormalities in ALS: correlating 7 Tesla MRI and pathology. PLoS One 7, e35241.

Mitsumoto, H., Ulug, A.M., Pullman, S.L., Gooch, C.L., Chan, S., Tang, M.X., Mao, X., Hays, A.P., Floyd, A.G., Battista, V., Montes, J., Hayes, S., Dashnaw, S., Kaufmann, P., Gordon, P.H., Hirsch, J., Levin, B., Rowland, L.P., Shungu, D.C., 2007. Quantitative objective markers for upper and lower motor neuron dysfunction in ALS. Neurology 68, 1402–1410.

Mori, S., Crain, B.J., Chacko, V.P., van Zijl, P.C., 1999. Three-dimensional tracking of axonal projections in the brain by magnetic resonance imaging. Annals of Neurology 45, 265–269.

Mori, S., Oishi, K., Jiang, H., Jiang, L., Li, X., Akhter, K., Hua, K., Faria, A.V., Mahmood, A., Woods, R., Toga, A.W., Pike, G.B., Neto, P.R., Evans, A., Zhang, J., Huang, H., Miller, M.I., van Zijl, P., Mazziotta, J., 2008. Stereotaxic white matter atlas based on diffusion tensor imaging in an ICBM template. NeuroImage 40, 570–582.

Murayama, S., Inoue, K., Kawakami, H., Bouldin, T.W., Suzuki, K., 1991. A unique pattern of astrocytosis in the primary motor area in amyotrophic lateral sclerosis. Acta Neuropathologica 82, 456–461.

Murphy, M.J., Grace, G.M., Tartaglia, M.C., Orange, J.B., Chen, X., Rowe, A., Findlater, K., Kozak, R.I., Freedman, M., Strong, M.J., Lee, T.Y., 2008. Cerebral haemodynamic changes accompanying cognitive impairment in primary lateral sclerosis. Amyotrophic Lateral Sclerosis 9, 359–368.

Nickerson, J.P., Koski, C.J., Boyer, A.C., Burbank, H.N., Tandan, R., Filippi, C.G., 2009. Linear longitudinal decline in fractional anisotropy in patients with amyotrophic lateral sclerosis: preliminary results. Klinische Neuroradiologie 19, 129–134.

Oishi, K., Faria, A., Jiang, H., Li, X., Akhter, K., Zhang, J., Hsu, J.T., Miller, M.I., van Zijl, P.C., Albert, M., Lyketsos, C.G., Woods, R., Toga, A.W., Pike, G.B., Rosa-Neto, P., Evans, A., Mazziotta, J., Mori, S., 2009. Atlas-based whole brain white matter analysis using large deformation diffeomorphic metric mapping: application to normal elderly and Alzheimer's disease participants. NeuroImage 46, 486–499.

Pringle, C.E., Hudson, A.J., Munoz, D.G., Kiernan, J.A., Brown, W.F., Ebers, G.C., 1992. Primary lateral sclerosis. Clinical features, neuropathology and diagnostic criteria. Brain 115, 495–520.

Pyra, T., Hui, B., Hanstock, C., Concha, L., Wong, J.C., Beaulieu, C., Johnston, W., Kalra, S., 2010. Combined structural and neurochemical evaluation of the corticospinal tract in amyotrophic lateral sclerosis. Amyotrophic Lateral Sclerosis 11, 157–165.

Reuter, M., Rosas, H.D., Fischl, B., 2010. Highly accurate inverse consistent registration: a robust approach. NeuroImage 53, 1181–1196.

Reuter, M., Schmansky, N.J., Rosas, H.D., Fischl, B., 2012. Within-subject template estimation for unbiased longitudinal image analysis. NeuroImage 61, 1402–1418.

Roccatagliata, L., Bonzano, L., Mancardi, G., Canepa, C., Caponnetto, C., 2009. Detection of motor cortex thinning and corticospinal tract involvement by quantitative MRI in amyotrophic lateral sclerosis. Amyotrophic Lateral Sclerosis 10, 47–52.

Rowland, L.P., 1999. Primary lateral sclerosis: disease, syndrome, both or neither? Journal of Neurological Sciences 170, 1–4.

Sach, M., Winkler, G., Glauche, V., Liepert, J., Heimbach, B., Koch, M.A., Buchel, C., Weiller, C., 2004. Diffusion tensor MRI of early upper motor neuron involvement in amyotrophic lateral sclerosis. Brain 127, 340–350.

Sage, C.A., Peeters, R.R., Gorner, A., Robberecht, W., Sunaert, S., 2007. Quantitative diffusion tensor imaging in amyotrophic lateral sclerosis. NeuroImage 34, 486–499.

Smith, S.M., Jenkinson, M., Woolrich, M.W., Beckmann, C.F., Behrens, T.E., Johansen-Berg, H., Bannister, P.R., De Luca, M., Drobnjak, I., Flitney, D.E., Niazy, R.K., Saunders, J., Vickers, J., Zhang, Y., De Stefano, N., Brady, J.M., Matthews, P.M., 2004. Advances in functional and structural MR image analysis and implementation as FSL. NeuroImage 23 (Suppl. 1), S208–S219.

Strong, M.J., Yang, W., 2011. The frontotemporal syndromes of ALS. Clinicopathological correlates. Journal of Molecular Neuroscience 45, 648–655.

Strong, M.J., Lomen-Hoerth, C., Caselli, R.J., Bigio, E.H., Yang, W., 2003. Cognitive impairment, frontotemporal dementia, and the motor neuron diseases. Annals of Neurology 54 (Suppl. 5), S20–S23.

Swash, M., Desai, J., Misra, V.P., 1999. What is primary lateral sclerosis? Journal of Neurological Sciences 170, 5–10.

Tartaglia, M.C., Rowe, A., Findlater, K., Orange, J.B., Grace, G., Strong, M.J., 2007. Differentiation between primary lateral sclerosis and amyotrophic lateral sclerosis: examination of symptoms and signs at disease onset and during follow-up. Archives of Neurology 64, 232–236.

Tartaglia, M.C., Laluz, V., Rowe, A., Findlater, K., Lee, D.H., Kennedy, K., Kramer, J.H., Strong, M.J., 2009. Brain atrophy in primary lateral sclerosis. Neurology 72, 1236–1241.

Thivard, L., Pradat, P.F., Lehericy, S., Lacomblez, L., Dormont, D., Chiras, J., Benali, H., Meininger, V., 2007. Diffusion tensor imaging and voxel based morphometry study in amyotrophic lateral sclerosis: relationships with motor disability. Journal of Neurology, Neurosurgery, and Psychiatry 78, 889–892.

Turner, M.R., Modo, M., 2010. Advances in the application of MRI to amyotrophic lateral sclerosis. Expert Opinion on Medical Diagnostics 4, 483–496.

Turner, M.R., Cagnin, A., Turkheimer, F.E., Miller, C.C., Shaw, C.E., Brooks, D.J., Leigh, P.N., Banati, R.B., 2004. Evidence of widespread cerebral microglial activation in amyotrophic lateral sclerosis: an [11C](R)-PK11195 positron emission tomography study. Neurobiology of Disease 15, 601–609.

Turner, M.R., Hammers, A., Allsop, J., Al-Chalabi, A., Shaw, C.E., Brooks, D.J., Leigh, P.N., Andersen, P.M., 2007. Volumetric cortical loss in sporadic and familial amyotrophic lateral sclerosis. Amyotrophic Lateral Sclerosis 8, 343–347.

Turner, M.R., Grosskreutz, J., Kassubek, J., Abrahams, S., Agosta, F., Benatar, M., Filippi, M., Goldstein, L.H., van den Heuvel, M., Kalra, S., Lule, D., Mohammadi, B., 2011. Towards a neuroimaging biomarker for amyotrophic lateral sclerosis. Lancet Neurology 10, 400–403.

Turner, M.R., Agosta, F., Bede, P., Govind, V., Lule, D., Verstraete, E., 2012. Neuroimaging in amyotrophic lateral sclerosis. Biomarkers in Medicine 6, 319–337.

Ulug, A.M., Grunewald, T., Lin, M.T., Kamal, A.K., Filippi, C.G., Zimmerman, R.D., Beal, M.F., 2004. Diffusion tensor imaging in the diagnosis of primary lateral sclerosis. Journal of Magnetic Resonance Imaging 19, 34–39.

Unrath, A., Muller, H.P., Riecker, A., Ludolph, A.C., Sperfeld, A.D., Kassubek, J., 2010. Whole brain-based analysis of regional white matter tract alterations in rare motor neuron diseases by diffusion tensor imaging. Human Brain Mapping 31, 1727–1740.

Vargas, M.R., Johnson, J.A., 2010. Astrogliosis in amyotrophic lateral sclerosis: role and therapeutic potential of astrocytes. Neurotherapeutics 7, 471–481.

Verstraete, E., van den Heuvel, M.P., Veldink, J.H., Blanken, N., Mandl, R.C., Hulshoff Pol, H.E., van den Berg, L.H., 2010. Motor network degeneration in amyotrophic lateral sclerosis: a structural and functional connectivity study. PLoS One 5, e13664.

Verstraete, E., Veldink, J.H., Hendrikse, J., Schelhaas, H.J., van den Heuvel, M.P., van den Berg, L.H., 2012. Structural MRI reveals cortical thinning in amyotrophic lateral sclerosis. Journal of Neurology, Neurosurgery, and Psychiatry 83, 383–388.

Wakana, S., Caprihan, A., Panzenboeck, M.M., Fallon, J.H., Perry, M., Gollub, R.L., Hua, K., Zhang, J., Jiang, H., Dubey, P., Blitz, A., van Zijl, P., Mori, S., 2007. Reproducibility of quantitative tractography methods applied to cerebral white matter. NeuroImage 36, 630–644.

Xue, R., van Zijl, P.C., Crain, B.J., Solaiyappan, M., Mori, S., 1999. In vivo three-dimensional reconstruction of rat brain axonal projections by diffusion tensor imaging. Magnetic Resonance in Medicine 42, 1123–1127.

Zhang, Y., Schuff, N., Woolley, S.C., Chiang, G.C., Boreta, L., Laxamana, J., Katz, J.S., Weiner, M.W., 2011. Progression of white matter degeneration in amyotrophic lateral sclerosis: a diffusion tensor imaging study. Amyotrophic Lateral Sclerosis 12, 421–429.

Ziemann, U., Winter, M., Reimers, C.D., Reimers, K., Tergau, F., Paulus, W., 1997. Impaired motor cortex inhibition in patients with amyotrophic lateral sclerosis. Evidence from paired transcranial magnetic stimulation. Neurology 49, 1292–1298.